ELSEVIER

Materials Science and Engineering A204 (1995) 43–47

MATERIALS SCIENCE & ENGINEERING A

# Microscopic investigations of the nanocomposite WGa

H. Wolf[a,*], H.G. Zimmer[a], T. Filz[a], St. Lauer[a], Th. Wichert[a], W. Krauß[b]

[a]*Technische Physik, Universität des Saarlandes, D-66041 Saarbrücken, Germany*
[b]*Institut für Werkstoffwissenschaften, Universität des Saarlandes, D-66041 Saarbrücken, Germany*

**Abstract**

The nanocomposite WGa was investigated by perturbed $\gamma\gamma$-angular correlation spectroscopy (PAC) using the probe atom $^{111}$In. The WGa samples were prepared by inert gas condensation; the Ga content ranged between 10 at.% and 50 at.%. The radioactive $^{111}$In atoms were diffused into the WGa samples at temperatures between 600 K and 740 K. Two distinct locations of the $^{111}$In probe atoms were observed. One was identified as a substitutional site within precipitated $\alpha$-Ga, for which a depression of the melting temperature was observed. The other was due to specific properties of the composite WGa and is stable up to temperatures of at least 500 K.

*Keywords:* Gallium; Tungsten; Nanocomposites

## 1. Introduction

The properties of nanostructured materials are mainly determined by the size of the crystallites and the interconnecting grain boundaries, as well as by their defect structures and, therefore, are evidently different from those of polycrystals of the same chemical composition. For example, the composite WGa cannot be formed by melting, because W and Ga do not form an alloy. Using the inert gas condensation technique [1], a nanocrystalline composite consisting of W and Ga can be formed, which has completely new properties, different from those of the constituents. While the technology for manufacturing nanocrystalline materials has been developed to some extent, a fundamental understanding of the special properties of nanocrystalline materials is still lacking [2]. Here, locally sensitive experimental techniques, like Mössbauer spectroscopy, EXAFS or perturbed $\gamma\gamma$-angular correlation (PAC), might be helpful in obtaining more information about grain boundaries, interfaces and defects within the formed crystallites.

This work presents PAC results obtained on nanocrystalline WGa composites that were produced by inert gas condensation and subsequently diffused with the radioactive PAC probe atoms $^{111}$In. In this way, new results were obtained which reflect specific properties of the composite WGa. The results observed in the produced WGa samples also include effects of the thermal diffusion treatment, such as a growth of the W particles, which were originally about 10 nm in diameter, and the precipitation of Ga. In principle, in-situ doping of the nanocomposite WGa with $^{111}$In should be possible in order to avoid the additional thermal treatment for radioactive doping. For technical reasons, PAC experiments on in-situ doped WGa samples will be the subject of future projects.

## 2. Experimental details

PAC spectroscopy commonly uses the radioactive probe atom $^{111}$In which decays to the excited level of its daughter isotope $^{111}$Cd (see Fig. 1). From this level two $\gamma$-quanta are emitted, thereby populating a spin $I = 5/2$ level with a half-life of 85 ns. The emission probability of the second $\gamma$-quantum with respect to the first one has a spatial anisotropy due to the conservation of the angular momentum during the decay process. This anisotropy is governed by the nuclear spins taking part in the decay process as well as by the multipolarities of the emitted $\gamma$-quanta. For the $\gamma\gamma$-cascade of the $^{111}$Cd nucleus the anisotropy is $A_2 = -0.14$. The $I = 5/2$ level has a nuclear quadrupole moment of $Q = 0.8$ b and is

* Corresponding author.


*SSDI* 0921-5093(95)09935-2

used for detecting the parameter of interest, namely the electric field gradient (EFG). The EFG is the second derivative of the electrostatic potential and, therefore, can be described by a second rank, traceless tensor. In its principal axis system this tensor is completely described by two quantities, namely its largest component $V_{zz}$ and the asymmetry parameter $\eta = (V_{xx} - V_{yy})/V_{zz}$, for which the relation $0 \leqslant \eta \leqslant 1$ holds if $|V_{xx}| \leqslant |V_{yy}| \leqslant |V_{zz}|$ is chosen. The hyperfine interaction of the quadrupole moment with the EFG at the site of the probe nucleus causes a threefold splitting of the $I = 5/2$ level, or in a classical framework, a periodic motion of the nuclear spin which leads to a modulation of the emission probability of the second $\gamma$-quantum. This modulation is governed by the three frequencies $\omega_1$, $\omega_2$, and $\omega_3 = \omega_1 + \omega_2$, resulting from the three possible energy differences of the split nuclear $I = 5/2$ state (see Fig. 1). The frequencies are proportional to the product $QV_{zz}$ and, therefore, are a measure of the strength of the EFG. The asymmetry parameter $\eta$ is determined by the ratio $\omega_2/\omega_1$ and the strength of the EFG is usually expressed by the quadrupole coupling constant $\nu_Q = eQV_{zz}/h$, which is proportional to $\omega_1$. In a PAC experiment, the second $\gamma$-quantum is recorded coincidentally with the first one, using two $\gamma$-detectors which are arranged under a fixed angle $\theta$. In general, four $\gamma$-detectors arranged along two orthogonal axes are used. This setup enables the simultaneous recording of 12 coincidence spectra, eight with a relative angle of 90° and four with a relative angle of 180°. By proper combination of the measured coincidence spectra the exponential decay function is eliminated [3] and the resulting modulation function can be written in the following way:

$$W(\theta,t) = 1 + P(\theta) \cdot R(t),$$

with

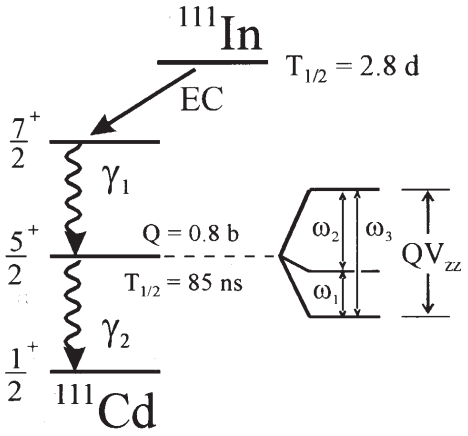


Fig. 1. Decay scheme of the PAC probe $^{111}$In/$^{111}$Cd. The incorporation of the probe atom in the sample is determined by the chemical properties of In, whereas the EFG is measured at the $I = 5/2$ level of $^{111}$Cd via the hyperfine interaction of the nuclear quadrupole moment $Q$ with the external EFG.

$$R(t) = A_2 \cdot \{f \cdot (s_0 + \sum_{n=1}^{3} s_n \cos\omega_n t) + (1 - f)\}$$

Here, $f$ denotes the fraction of probe atoms within an environment, producing a particular non-zero EFG, and $(1 - f)$ is the fraction of the remaining probe atoms without an EFG. The angular dependent function $P(\theta)$ corresponds to the second-order Legendre polynominal $P_2(\cos\theta)$ in the case of a polycrystalline sample. If there are different environments surrounding the probe atoms and producing different EFGs, $f$ will be split into different fractions $f(i)$, whereby each one is represented by its own characteristic frequency triplet $\omega_n(i)$. The total amount of $^{111}$In necessary for a PAC experiment is of the order of $10^{11}$ atoms, therefore the resulting volume concentration of probe atoms within the investigated sample is very low, in general. Typically, one gets concentrations of $10^{14}$–$10^{17}$ cm$^{-3}$, depending on the distribution of the probe atoms within the sample. More details on the PAC technique can be found for example in Ref. [3].

The origin of an EFG, existing at the site of the probe atom, can be either a non-cubic structure of the host lattice, or the formation of defect complexes including the probe atom. Strength, asymmetry, and orientation of the EFG tensor with respect to the host lattice are determined by the ratio of the lattice constants, in the case of non-cubic crystals. For example, the orthorhombic Ga lattice produces a non-axially symmetric EFG ($\nu_Q = 142$ MHz, $\eta = 0.2$) at the substitutional lattice site [4], whereas the EFG of the bcc W lattice is zero at substitutional lattice sites. The second case is the agglomeration of one or more defects (impurities or intrinsic defects) about the probe atom. The strenght of an EFG as produced by defect complexes decreases rapidly with the distance of the defects to the probe atom; the maximum distance of a detectable defect corresponds to about 1–2 lattice constants. Asymmetry and orientation of the EFG tensor are determined by the geometrical structure of the formed defect complex. In W, the EFG belonging to different defect complexes, which include trapped vacancies or impurity atoms, are well known [5,6].

## 3. Results and discussion

The WGa samples investigated by PAC were prepared by inert gas condensation and subsequently compacted into pellets of 8 mm diameter with a thickness of about 0.5 mm. The Ga content of the used samples ranged between 10 at.% and 50 at.%. The size of the W particles was about 10 nm as determined by X-ray diffraction measurements. By measuring the specific heat as a function of temperature (DSC) no precipitated Ga was detected. Subsequently, pieces of about 3

Table 1
WGa samples investigated by PAC spectroscopy in this work. The Ga content, the diffusion conditions for the respective sample, the transition rate of $^{111}$In after diffusion and the population of the resulting local environments by the probe atoms are given. In general, the data for $f_{Ga}$, $f_{WGa}$, $f_0$ and $f_r$ were evaluated at 77 K; for samples 3, 5 and 10, the temperature was 295 K

| Sample | at.% Ga | $T_{diff}$ (K)/$t_{diff}$ (h) | $^{111}$In rate (%) | $f_{Ga}$ (%) | $f_{WGa}$ (%) | $f_0$ (%) | $f_r$ (%) |
|---|---|---|---|---|---|---|---|
| 1 | 10–15 | 600/1,5 | 60 | 0 | 0 | 12 | 88 |
| 2 | 10–15 | 600/2 | 55 | 0 | 0 | 10 | 90 |
| 3 | 40–50 | 593/1,5 | 11 | 0 | 0 | 7 | 93 |
| 4 | 40–50 | 708/16 | 55 | 21 | 14 | 8 | 57 |
| 5 | 40–50 | 700/25 | 1 | 0 | 0 | 0 | 100 |
| 6 | 40–50 | 697/16,3 | 53 | 3 | 14 | 0 | 86 |
| 7 | 40–50 | 740/16,6 | 66 | 36 | 0 | 0 | 63 |
| 8 | 33 | 740/16,5 | 63 | 5 | 0 | 0 | 95 |
| 9 | 33 | 739/4 | 70 | 9 | 0 | 4 | 87 |
| 10 | 33 | 739/4 | 70 | 0 | 0 | 14 | 86 |

mm$^3$ were cut from those pellets and diffused with the radioactive $^{111}$In atoms. The Ga content of the investigated samples and the conditions used for diffusion are listed in Table 1. Additionally, this table contains the transition rates of $^{111}$In atoms, which were achieved during the diffusion process, and information about the observed EFG. Note that the variations in the observed fractions, obtained for equivalently treated samples, are not systematic, although the conditions for diffusion with the $^{111}$In probe atoms were comparable. Obviously, the ex-situ doping by diffusion is not easily reproducible, so that in-situ doping during inert gas condensation should be envisioned for future experiments. The size of the W paricles was enlargered to about 30 nm due to thermal treatment and, at the same time, precipitated Ga was observed by DSC measurements. For some of the samples, the probe atoms are observed to be incorporated within crystalline Ga as is recognized by the non-axially symmetric EFG ($\nu_Q = 142$ MHz, $\eta = 0.2$ at $T = 77$ K), which is well known for $^{111}$In/$^{111}$Cd in Ga metal [4]. This fraction rises to $f_{Ga} = 36\%$ for sample 7. A second EFG ($\nu_Q = 295$ MHz, $\eta = 0$), observed for example in sample 4 was not known until now, neither in Ga nor in W, and reaches a population of $f_{WGa} = 30\%$. In Fig. 2(a), the PAC spectrum recorded for sample 4 at a temperature of $T = 14$ K is plotted, showing both the EFG due to Ga precipitates ($f_{Ga}$) and the new, axially symmetric EFG ($f_{WGa}$), which is interpreted as being connected to specific properties of the composite WGa. The small EFG distribution, indicated by the small damping of the $R(t)$ spectrum, requires a highly ordered structure around these probe atoms, and the axial symmetry of the EFG indicates a local hexagonal or tetragonal structure. For the same sample, the PAC spectra in Figs. 2(b) and (c) show that only the axially symmetric EFG, belonging to $f_{WGa}$, is present at higher sample temperatures.

In order to obtain more information about the composite WGa, the temperature dependences of the EFG and of the associated populations of the different locations in the range 14 K $< T <$ 500 K were investigated. Four different locations of probe atoms could be distinguished during the PAC experiments in the composite WGa; the temperature dependences of their populations are plotted in Fig. 3. Besides the fractions $f_{Ga}$ and $f_{WGa}$, some of the probe atoms are $f_0$ located in an environment without an EFG, corresponding to the time-independent part of the $R(t)$ spectrum, e.g. in Fig. 2(c). Finally, some of the probe atoms reside in an undefined environment ($f_r$), in which the associated EFG produces frequencies that are too high to be resolved by the $\gamma$-detectors. Therefore, the value of $f_r$ was determined by the condition that all fractions have to sum to 100%. Below 250 K, the fraction $f_{Ga}$ remains almost constant and vanishes above $T = 288$ K (compare Fig. 2(b)). At the same time, the fraction $f_0$ increases from 0% to 50% and, in addition, the fraction

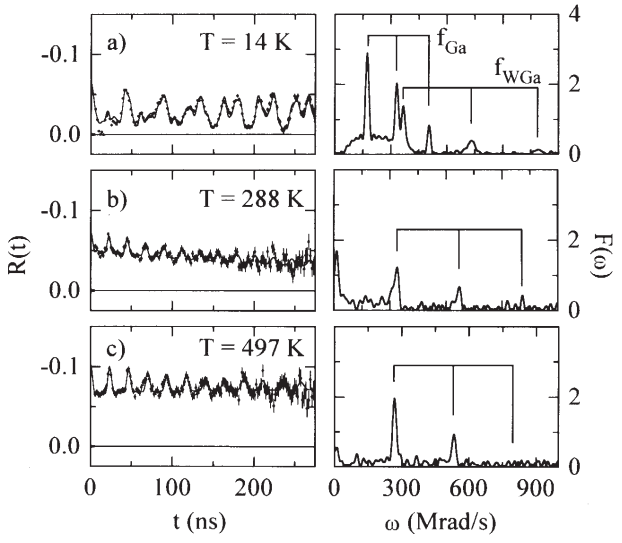


Fig. 2. PAC time spectra and their Fourier transforms for sample 4, recorded for different sample temperatures. They show the typical EFG for Ga precipitates (a) and the composite WGa (a)–(c).

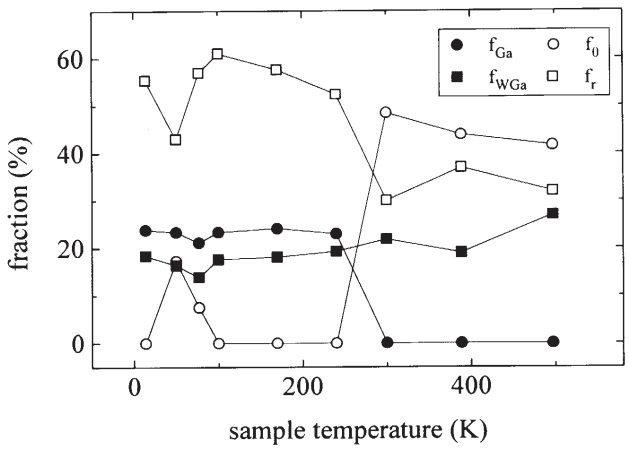


Fig. 3. The temperature dependence of the population of the four detected locations of the probe atom In for sample 4. The disappearance of $f_{Ga}$ between 240 K and 288 K is caused by the melting of the precipitated Ga matrix.

$f_r$ decreases from 50% to 30%. (The exchange between $f_0$ and $f_r$ at $T = 50$ K is not understood, but is possibly due to an experimental artifact.) The disappearance of $f_{Ga}$ and the decrease in $f_r$ are attributed to the melting of the precipitated crystalline Ga matrix. At the same time, the decrease in $f_{Ga}$ and $f_r$ shows that about one-half of the $^{111}$In atoms within the Ga precipitates are located on substitutional sites of crystalline $\alpha$-Ga. The second result is the reduction in the melting temperature from 302 K for pure Ga down to a temperature between 240 K and 288 K for the observed Ga precipitates. A similar observation was made on a thermally treated WGa sample by DSC measurements. The depression of the melting temperature within nanocrystalline compounds has been observed for different materials and is explained by the size dependence of the thermal vibrations of the matrix atoms [7]. A better quantitative determination of the depression of the melting temperature of precipitated Ga is the subject of current experiments. For sample 9 this temperature range was narrowed down to an interval between 240 K and 260 K.

The fraction $f_{WGa}$ remains almost constant up to a temperature of 400 K and increases irreversibly at higher temperatures. Such an increase, being caused by the sample treatment at higher temperatures, is shown for sample 6 in Fig. 4. After diffusion of the probe atoms $^{111}$In, $f_{WGa}$ reaches 10% but increases to 38% after annealing at $T_a = 690$ K for 5 h. At present, the maximum population of $f_{WGa}$ that can be reached under favourable conditions is not known. The fact that the crystalline environment causing $f_{WGa}$ has been thermally stable during PAC experiments up to temperatures far above the melting point of $\alpha$-Ga, clearly shows that this environment does not correspond to precipitated Ga. The measured value of the EFG is difficult to use to obtain direct information about the local environment of the probe atom, for theoretical reasons. For the origin of the EFG, three possibilities can be considered. First, the In atoms might be located at interfacial sites within a well-defined surrounding that is not affected by the melting of the precipitated Ga. Second, an intermetallic compound of W and Ga with a hexagonal or tetragonal lattice structure might have been formed in which the In atoms are located at well-defined lattice sites. This compound must be stable up to temperatures of at least 500 K. Third, the In atoms might have diffused into W particles and the observed EFG could be due to a defect complex in the W lattice involving the probe atom $^{111}$In. The latter possibility would be very surprising because the diffusion of $^{111}$In into polycrystalline W samples should not occur at such low temperatures used for the present sample treatment (see Table 1). A conclusive interpretation of the local structure corresponding to $f_{WGa}$ is still lacking and will require more experimental data from complementary experimental techniques.

In general, the temperature dependence of the EFG also yields information about possible environments for the probe atoms. In Fig. 5, the temperature dependences of the EFG belonging to $f_{WGa}$ and $f_{Ga}$ show a continuous decrease when plotted versus $T^{3/2}$. The temperature dependence of the EFG in non-cubic metals has been extensively studied in the past and in many cases a $T^{3/2}$ dependence was found, which is explained by the thermal excitation of phonons [8]. The temperature dependence of the EFG measured in the crystalline Ga precipitates follows the $T^{3/2}$ behaviour known for $\alpha$-Ga metal. For the EFG on metal surfaces, a rather linear temperature dependence can be expected, taking into account the properties of the phonon spectrum of a two-dimensional solid [9]. The decrease in the EFG corresponding to $f_{WGa}$ in the range between $T = 14$ K and $T = 500$ K seems to follow neither a $T^{3/2}$ dependence (Fig. 5) nor a linear $T$ dependence. A detailed interpretation of the observed temperature dependence of $f_{WGa}$ has to await further theoretical work.

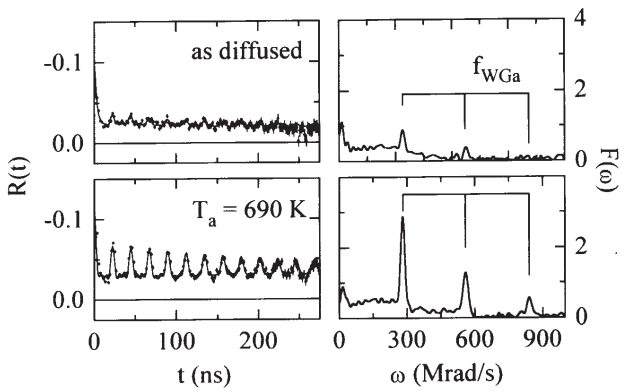


Fig. 4. The influence of heat treatment on the population of the site $f_{WGa}$.

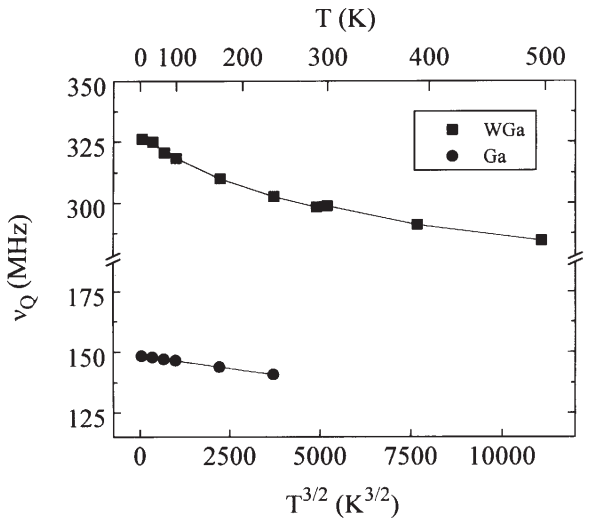


Fig. 5. Temperature dependences of the EFG corresponding to $f_{Ga}$ and $f_{WGa}$. In contrast to $f_{Ga}$, $f_{WGa}$ does not follow a $T^{3/2}$ law.

## 4. Conclusion

From PAC experiments on the nanocomposite WGa two results were obtained. First, the precipitation of Ga as a consequence of the growth of the W particles was deduced from the observation of the EFG of the orthorhombic lattice structure of $\alpha$-Ga. The melting temperature of the precipitated Ga is evidently reduced and was determined to be in the temperature range between 240 K and 260 K for a WGa sample containing 33 at.% Ga. Second, a new EFG was detected which is typical of the composite WGa, and during the PAC investigations this structure was stable up to temperatures of at least 500 K. The exact local structure corresponding to this EFG is still unknown but some possible interpretations were proposed. The question of the extent to which the local structures observed were affected by ex-situ doping of the samples with $^{111}$In probes at temperatures above 600 K, will be subject of future experiments. There, in-situ doping of the WGa samples with $^{111}$In atoms during inert gas condensation is envisaged.

## Acknowledgements

Financial support by the Deutsche Forschungsgemeinschaft within the Sonderforschungsbereich 277 at the Universität des Saarlandes is gratefully acknowledged

## References

[1] H. Gleiter, *J. Appl. Cryst.*, *24* (1991) 79.
[2] R.D. Shull, *Nanostructured Mater.*, *2* (1993) 213.
[3] Th. Wichert, M. Deicher, G. Grübel, R. Keller, N. Schulz and H. Skudlik, *Appl. Phys.*, *A 48* (1989) 59.
[4] W. Keppner, W. Körner, P. Heubes and G. Schatz, *Hyp. Int.*, *9* (1981) 293.
[5] J.R. Fransen, M.S. Abd El Keriem and F. Pleiter, *J. Phys. Condens. Matter*, *3* (1991) 9871.
[6] M.S. Abd El Keriem, D.P. van der Werf and F. Pleiter, *Phys. Rev.*, *B 47* (1993) 14771.
[7] F.G. Shi, *J. Mater. Res.*, *9* (1994) 1307.
[8] K. Nishijama, F. Dimmling, T. Kornrumpf and D. Riegel, *Phys. Rev. Lett.*, *37* (1976) 956.
[9] T. Klas, R. Fink, G. Krausch, R. Platzer, J. Voigt, R. Wesche and G. Schatz, *Surf. Sci.*, *216* (1989) 270.